Geological Journal

A Middle Miocene carbonate embankment on an active volcanic slope: Ilhéu de Baixo, Madeira Archipelago, Eastern Atlantic

Journal:	*Geological Journal*
Manuscript ID:	GJ-12-0104.R1
Wiley - Manuscript type:	Research Article
Date Submitted by the Author:	n/a
Complete List of Authors:	Baarli, B. Gudveig; Williams College, Geosciences Cachão, Mario; Universidade de Lisboa, Geologia e Centro de Geologia da Silva, Carlos; Universidade de Lisboa, Geologia e Centro de Geologia Johnson, Markes; Williams College, Geosciences Mayoral, Eduardo; Universidad de Huelva, Geodinámica y Paleontología Santos, Ana; Universidad de Huelva, Geodinámica y Paleontología
Keywords:	Carbonates, coralline red algae (rhodoliths), Middle Miocene (Langhian-Serravallian), density flows, volcaniclastic apron, Madeira Archipelago, corals

A Middle Miocene carbonate embankment on an active volcanic slope: Ilhéu de Baixo, Madeira Archipelago, Eastern Atlantic

*B. GUDVEIG BAARLI**[1], *MÁRIO CACHÃO*[2], *CARLOS M. DA SILVA*[2], *MARKES E. JOHNSON*[1], *EDUARDO J. MAYORAL*[3], and *ANA SANTOS*[3]

[1] *Department of Geosciences, Williams College, USA*

[2] *Faculdade de Ciências da Universidade de Lisboa, Departamento de Geologia e Centro de Geologia, Portugal*

[3] *Departamento de Geodinámica y Paleontología, Facultad de Ciencias Experimentales, Universidad de Huelva, Spain*

Corresponding author; E-mail address: gbaarli@williams.edu

Department of Geosciences, Williams College, 947 Main Street, Williamstown, MA 01267 USA

Office phone: 01-413-597-2329; Fax: 01-413-597-4116

Carbonate factories on insular oceanic islands in active volcanic settings are poorly explored. This case study illuminates marginal limestone deposits on a steep volcanic flank and their recurring interruption by deposits linked to volcaniclastic processes. Historically known as Ilhéu da Cal (Lime Island), Ilhéu de Baixo was separated from Porto Santo, in the Madeira Archipelago, during the course of the Quaternary. Here extensive mines were tunnelled in Miocene carbonate strata for the production of slaked-lime. Approximately 10,000 m^3 of calcarenite (-1 to 1 ø) were removed by hand labour from the Blandy Brothers mine at the south end of the islet. Investigations of two

stratigraphic sections at opposite ends of the mine reveal that the quarried material represents an incipient carbonate ramp developed from east to west and embanked against the flank of a volcanic island. Petrographic analysis of limestones from the mine show that coralline red algae from crushed rhodoliths account for 51% of all identifiable bioclasts. This material was transported shoreward and deposited on the ramp between wave base and storm wave-base at moderate depths. The mine's roof rocks are formed by surtseyan deposits from a subsequent volcanic eruption. Volcaniclastic density flows also are a prevalent factor interrupting renewed carbonate deposition. These flows arrived downslope from the north and gradually steepened the debris apron westwards. Slope instability is further shown by a coral rudstone density flow that followed from growth of a coral reef dominated by *Pocillopora madreporacea* (Lamarck), partial reef collapse, and transport from a more easterly direction into a fore-reef setting. The uppermost facies represents a soft bottom at moderate depths in a quiet, but shore- proximal setting. Application of this study to a broader understanding of the relationship between carbonate and volcaniclastic deposition on oceanic islands emphasizes the susceptibility of carbonates to dilution and complete removal by density flows of various kinds, in contrast to the potential for preservation beneath less disruptive surtseyan deposits.

KEY WORDS carbonates; corals; coralline red algae (rhodoliths); density flows; Middle Miocene (Langhian-Serravallian); volcaniclastic apron; Madeira Archipelago

1. INTRODUCTION

Accumulation of carbonate sediments has long been recognized as forming part of a dynamic, multi-faceted system with deep roots in the geological record (Wilson, 1975; Scholle *et al*., 1983). Despite early contributions by Darwin (1839, 1844) on coastal limestone deposits from Santiago in the Cape Verde Islands, the standard literature on carbonates provides few observations on non-reef deposits around volcanic islands. For example Soja (1993) noted the widespread misconception that conditions must have been unfavourable for the development and "preservation of carbonates in environments surrounding active volcanic arcs and other island chains located in isolated parts of ocean basins." More recently, there have appeared a host of papers on such carbonate deposits, most of them used as markers for eustasy and uplift on oceanic islands in the Cape Verde Islands (Zazo *et al.,* 2007; 2010), Canary Islands (Zazo *et al.,* 2002; Meco *et al.,* 2007) and the Azores (Ávila *et al.,* 2009). Submerged lava aprons with steep underwater slopes are commonly generated by emerging oceanic island systems. Such systems have been investigated regarding patterns of volcaniclastic deposition (Watton *et al.,* 2013). Comparatively little is known, however, about carbonates preserved between eruptive episodes and reactivation of lava flows.

The Portuguese island of Porto Santo and two of its associated islets (Ilhéu de Baixo and Ilhéu de Cima, Fig. 1) in the Madeira Archipelago (North Atlantic Ocean) exhibit Middle Miocene (Langhian-Serravallian) limestone accumulations that record a wide range of palaeoecological settings contemporaneous with active oceanic volcanism. Previous studies have focused on Ilhéu de Cima, the southeastern islet with a hurricane deposit dominated by unusually large rhodoliths on one flank (Johnson *et al*., 2011) and more sheltered rocky shores with variable biotas including a small fringing reef, as well

as encrusting red algae, corals and bivalves, boring bivalves, barnacles and boring barnacles together with localized *in situ* rhodoliths on the opposite flank (Santos *et al*., 2011 and Santos *et al*., 2012a, b, c). Ilhéu de Baixo (also known as Ilhéu de Cal or Lime Islet) was the site of earlier studies on a Miocene coral reef (Chevalier, 1972; Boekschoten and Best, 1981; Best and Boekschoten, 1982). Coral rudstone crops out at more than one stratigraphic level on the island, but it was other calcarenites that sustained the local mining industry for production of slaked lime during the mid-1800s to mid-1900s. The openings to an extensive network of mine tunnels remains easily visible at multiple levels around the islet.

During our investigation of the Blandy Brothers mine at the south end of Ilhéu de Baixo, a cursory examination by hand lens of rock samples from surviving mine pillars suggested that crushed rhodolith debris contributed to at least some of the mine's product. Finding the composition and sedimentary origins of the calcarenite was the starting impetus for this study, which was expanded to include corollary investigations on the depositional setting of coral rudstones and other limestone deposits above the stratigraphic level of the mine. Volcaniclastic layers and basalt flows fully dominate the bulk of Ilhéu de Baixo and underscore the additive construction of volcanic components from a nearby source. Thus, a further goal of this study is to understand the dynamics under which the more limited limestone deposits preserved on the island were incorporated with coeval volcanic by-products on the flanks of an active oceanic volcano.

2. LOCATION AND GEOLOGICAL SETTING

The Madeira Archipelago is situated 650 km off the northwest coast of Africa in the North Atlantic Ocean. Porto Santo is an outlying island located 50 km northeast of the principal island of Madeira (Fig. 1). The geological map by Ferreira (1996) covers Porto Santo and several satellite islets, at a scale of 1:25,000. The volcanic succession in the eastern part of Porto Santo is described by Schmidt and Schmincke (2002). That part of the island features an older trachytic volcanic edifice unconformably overlain by hawaiitic flows, mostly submarine in disposition and emplaced prior to 12.5 Ma. Overall, this pattern agrees with the geological cross-section from Ferreira (1996) at Ilhéu de Baixo that shows dominant submarine basalt flows with intercalated hyaloclastites and reefal limestone dated to 15.2 Ma, but cut by a volcanic neck dated to 12.3 Ma. Thus, available radiometric dates support a Middle Miocene age (Langhian or earliest Serravallian) in close agreement with the biostratigraphy of calcareous nannofossils recovered from Lombinhos in eastern Porto Santo (Cachão *et al*., 1998).

The volcanic succession on Porto Santo is uplifted and was at one time part of a shoaling to emergent seamount (Schmidt and Schmincke, 2002). The largest islet is Ilhéu de Baixo separated by 0.5 km from the southwest corner of Porto Santo. With a circumference of 7 km, the north-south elongated islet covers an area approximately 1.5 km^2, much of which rises abruptly to a plateau more than 150 m above sea level. From the geometry of the volcanic and volcaniclastic units and the cartographic interpretation of Ferreira (1996), the Baixo sequence must be the youngest of the present-day preserved Miocene units. Schmidt and Schmincke (2002, p. 594) studied the eastern portion of Porto Santo but state generally that "facies architectures indicate emplacement on a gently sloping platform in southwestern Porto Santo."

A 65-m-thick sequence of volcaniclastic and fossil-bearing limestone beds are exposed at Paredes and Forno on the east side of Ilhéu de Baixo, as summarized by Silva (1959) and Mitchell-Thomé (1974). The reef limestone with the dominant coral *Pocillopora madreporacea* is from a lens-like deposit 1.6-m-thick, sitting on volcaniclastic rocks 45 m above sea level (Boekschoten and Best, 1981; Best and Boekschoten, 1982). The interbedded submarine basalt flows, volcaniclastic sediments, and fossil-bearing limestone beds discussed in this study are younger than the horizontal reef limestone at Paredes and Forno previously described by Boekschoten and Best (1981). The section is accessible from a landing site at the extreme south end of Ilhéu de Baixo via a route leading to the mine portal above Engrade Pequena on the west side of the island (Figs. 1 and 2). At a level about 50 m above sea level, the investigated units may be traced from one side of the island to the other over a distance of 65 m, in part directly through the mine galleries.

Today, the roof rock over the mine galleries is supported by about 25 intact pillars, roughly square in plan, generally about 15 m in circumference, and from 1.6 m to 2.5 m in height. The floor plan of the mine covers a total area of 5,259 m^2 (Fig. 2) and it can be estimated approximately 10,000 m^3 of limestone was extracted by hand labour over the mine's working lifetime. Volcaniclastic strata form the roof rock.

4. METHODS

Graphic lithological logs modified after the standard format used by the Shell Oil Company were compiled through strata adjacent to and above portals outside the Blandy

Brothers mine on both the west and east sides of Ilhéu de Baixo. Care was taken to register occurrences of trace fossils in addition to macrofossils.

Within the mine, four rock samples were collected at strategic locations for preparation of thin sections using a combination of large (5 cm x 7.5 cm) and standard (3 cm x 2 cm) slides. The percentage of bioclast and abiogenic clast components in each sample was determined by counting 400 points per side at 0.5-mm intervals using a mechanical stage on the petrographic microscope. Three trials were conducted for each slide in order to test the reliability of the counts. These parameters were chosen so as to maximize accuracy and confidence in calculation of average percentages according to the guidelines of Van der Plas and Tobi (1965). Because voided spaces due to dissolution were encountered in all samples and because micrite proved problematic as to specific biological origins, a subset of data was tabulated to show the average percentages among all identifiable bioclasts in each sample.

With regard to the prominent stratum of coral rudstone above the mine, coral identification was based on the surveys of Boekschoten and Best (1981) and Best and Boekschoten (1982). In order to test the possible degree of post-mortem transport, a compass was used to measure the orientations of the long axes of 100 coral colonies larger than 15 cm in diameter exposed in the cliff face on the west side of the island and another 100 from the same stratum on the east side of the island. The mean direction of corallum growth was measured starting from the youngest (smallest) part of the colony as pointed on a midline towards the centre of the oldest (largest) part of the colonies. Sample quadrates of 20×20 cm were used to collect quantitative data on trace-fossil content preserved on the coral surface.

5. FACIES DEFINITIONS AND RELATIONSHIPS

5.1. Stratigraphic overview

Seen from the sea, the east side of Ilhéu de Baixo provides an excellent cross-section of the overall stratigraphic succession (Fig. 3A). Carbonate layers discerned as thin, light-coloured carbonate bands are extensively mined (white arrows on Fig. 3B). Intercalated between the carbonates are dark-coloured volcaniclastic wedges that thicken strongly towards the north (Black arrow, 2, Fig. 3B). The same kind of sequence is seen even further north, sloping in the opposite direction. Many of the volcaniclastic beds terminate near the south end of the island (Fig. 3C). This study is concerned with the youngest sediment package found at the southern end of the island (Black arrow 1, Fig. 3B, section between the white arrows in Fig. 3C). The section is sandwiched between layers of matrix-supported hyaloclastite and pillow breccia with isolated pillows (following the classification of Watton *et al*., 2013) and a 7-m-thick layer of pillow basalt. It starts with the lowest, mined carbonate seam (Fig. 3D and E), followed by volcaniclastic conglomeratic layers and renewed limestone deposition (between the arrows in Fig. 3C). Stratigraphic logs show that the succession can be divided into four facies (Fig. 4) as described below.

5.2. Facies I: Fine-grained massive carbonates

Facies I consists of massive, medium to well-sorted and medium- to very coarse-grained carbonates (wackestone to packstone). The lithic content is low and decreases upwards. Whole fossils are scarce and floating in the matrix. Rare macrofossils include whole and fragmented rhodoliths, scattered pectinid bivalves and gastropods. The contact with the underlying bed is not exposed in an accessible profile. Photographs of the vertical cliff on the west section (Fig. 3C) indicate that the limestone rests on mixed submarine pillow lava, pillow breccia, and hyaloclastites. The measured strike (210 ^{o}) and dip (9^{o}) is to the SSW (e.g. very close to the orientation between the two measured sections).

The east section exposes a profile close to the full thickness of the bed (3 m), while in the west section the lower parts are obscured by mining debris (Fig. 4). Very coarse-grained carbonate sand with a few floating, well-rounded basalt cobbles are seen in the east section, while the west section reveals medium-grain size carbonate without basalt clasts and a poorly diverse ichno-assemblage consisting of *Bichordites* isp. and *Dactyloidites* isp. in the upper part of the bed.

Four thin sections were sampled from the middle level of the limestone bed; two come from the west side, one in the middle of the mine, and another from the east side The four counts are remarkably similar (Tables 1-4) and are, therefore, treated jointly. Micrite is the dominant component (>50%). The wackestone to packstone is characterized by well-rounded red algal grains (~ 50% of the bioclastic grains), frequently surrounded by micritic rims or envelopes (Figs. 5A, B black arrow). Fragments of bivalves (Fig. 5A) are common, while coral fragments, foraminifers and echinoderm fragments are frequent. Gastropods occur mainly as ghosts surrounded by sparry micrite. Rare bryozoans and serpulids are also present. Identified foraminifers are

benthic forms such as *Textularia* sp., *Amphistegina* sp., and unidentified rotaliids (Figs. 5C, D, E,). The bioclasts, together with unsorted angular to subangular basalt clasts, are grain supported for the most part, interspersed with areas more rich in micrite. The only clear difference between the east and west ends of this unit is a decrease in grain size from east to west and a lower percentage of voids in the middle of the mine.

5.3. Facies II: Conglomeratic tuffs and tuffites

Facies II (Fig. 4) consists of tuffs, tuffites, and thick-bedded conglomeratic beds with a predominantly volcaniclastic matrix. The clasts are mainly basalt, but tuff also is common. Clast-size varies strongly between beds (Figs. 3D top, 6A, B) and laterally within beds. Finer grained beds are often thin to very thin-bedded and may lack erosive bases. Imbrication of larger clasts can be observed in some of them. Dish and flame structures are common near the base of many beds (Fig. 6B, arrow 1) and the bases are often erosive. Some of the coarser conglomeratic beds show reversed grading and large, angular to rounded boulders at the top, projecting into the overlying layer (Fig. 6B, white arrow 2). Scattered, marine fossils occur throughout the layer.

In the east section (Fig. 4), large basalt boulders at the top of beds and more rarely within beds, are encrusted by oysters, *Spondylu*s sp., serpulids, and bryozoans (Figs. 6B, C). Oysters are also common floating in the matrix. Encrusted blocks are not seen on the west side. The west section, however, displays thin, graded, rhythmic beds and flatly laminated to thinly bedded layers in between and lateral to the coarser conglomeratic beds. There is a pronounced fining of beds southwards. This is well observed in the first

bed above Facies I laying conformably on the carbonates (Fig. 6A). *Clypeaster* sp. and pectinid bivalves occur in the upper layer of this facies.

5.4. Facies III: Exotic boulders and coral rudstone

Facies III consists of carbonates with about 30% lithic content. The lower bed is a flatly laminated and strongly recrystallized, coarse-carbonate sand (grainstone). It incorporates mainly small basalt clasts and bioclasts (Figs. 6D, E, lower bed). The overlying thick bed is a coral rudstone that contains mostly angular and eroded cobbles and boulders of corals, chaetetid sponges, and large clasts of basalt floating in a poorly sorted granular carbonate matrix (Figs. 6D, upper bed, and 6F). Both the coral heads and the sponges tend to be conical in shape, reflecting whole heads and broken branches of large corals. Growth directions of corals were measured near both stratigraphic sections. Rose diagrams (Fig. 7) show a majority of the coral colonies lying sidewise pointing upslope or downslope, while the rest are either in upright position, or rarely, upside down. The corals *Pocillopora madreporacea* (Lamarck) and *Tarbellastrea reussiana* (Milne-Edward and Haime) are most commonly represented. Many are bored by pholad bivalves, which occurred both during active growth and after the corals were dead (Fig. 8A). The bivalve *Lithophaga (Leiosolenus)* sp. sometimes occurs in *G. hospitium* Kleemann (Figs. 8A arrow 2, 8B and 8C, black arrows). The ichnotaxon *Gastrochaenolites orbicularis* Kelly and Bromley appears most commonly (Fig. 8C, white arrow), sometimes with the body fossil *Jouannetia* sp. within the boring (Fig. 8A arrows 1). Many of these borings gave rise to geopetals showing that the tilt of the

overall sedimentary unit is mainly synsedimentary. Some chaetetid sponge heads are found encrusted on basalt boulders (Fig. 8D).

On the east side, a bioeroded exotic block measuring 1.60 x 0.95 m occurs in the lower laminated layer together with abundant casts of bivalves (Fig. 6D). The borings occurring in the block are *Gastrochaenolites lapidicus* Kelly and Bromley and *G. torpedo* Kelly and Bromley (Fig. 6E). The overlying coral rudstone shows more basalt cobbles within the bed on the east side compared with the west side, especially near the base and the top. Due to the steepness of the cliff face, lateral relations are difficult to discern on the east side. The measured logs of this facies on both sides are very similar (Figs. 4A, 4B). However, looking north on the west side, it is possible to see a wedge-shaped, conglomeratic and volcaniclastic bed inserted within Facies III, between the lower bed and the coral rudstone bed (Fig. 6F, below white arrow). The wedge has been eroded away by the coral rubble in the measured section, but reappears as a thin band below the coral rudstone further to the south. The rudstone bed thins to the north and south. A similar thinning and thickening is apparent on the east side. The overlying Facies IV occurs lateral to the termination of the coral bed (Fig. 6F, white arrow).

5.5. Facies IV: Calcareous volcaniclastic sand

This facies is a massive, poorly sorted, medium- to coarse-grained volcaniclastic sand with high carbonate content, wackestone to packstone, (Figs. 4 and 8E). Facies IV is not accessible on the east side. However, the unit there is fairly thin with a uniform thickness and a similar red colour to the fine-grained volcaniclastic beds below. Facies IV is well

exposed on the west side, both in the logged section and as a large bedding surface further south. There is a diverse but scattered fossil fauna consisting of rhodoliths and pectinid bivalves mixed with *Pinna* sp., *Spondylus* sp., echinoderm spines and tests, and also coral heads (Fig. 8F).

The large (540 m^2) bedding plane 40 m south of the measured section (Fig. 8G) with a dip of 20° SW reveals numerous tests, spines, and trace fossils from irregular echinoids such as *Clypeaster* sp. and *Spatangus* sp. The bivalves *Isognomon* sp., *Spondylus* sp. and *Pinna* sp. and the gastropod *Conus* sp. also are common. Towards the northern end of the bedding plane occur small (<50 cm in diameter) patches of corals encrusted by *Spondylus* sp. and serpulids showing a mix of coral heads in upright position and lying sideways (Fig. 8F). These corals are strongly bored. The bivalve borings are arranged sub-perpendicular and sub-horizontal to the coral surface and some of them demonstrate so-called calcareous false floors. Counts from 11 sampling grids (20×20 cm) yielded an average number of 8.8 *G. torpedo* per grid (97 specimens total) and 11.8 *G. hospitium* per grid (130 specimens total). Pillow lava and pillow breccia cap both sections.

6. FACIES INTERPRETATIONS

Figure 3B shows a strong presence of hyaloclastites and other volcaniclastic sediments interspersed with thin basalt layers that point to a volcano in the vicinity to the NNE. Figure 3C, depicting the studied section, demonstrates how the slope became progressively steepened. All the units investigated include marine fossils with marine

trace fossils found both in the basal and top layers that indicate the sequence was deposited in a submarine setting on the flank of a volcano. The studied section was deposited in a prograding prodelta to distal delta front, and no passage zone is preserved in the lava sequence above. However, approximately 7-m-thick pillow lava flows immediately overlying the section indicate the minimum absolute depositional depth for the sediments at the top.

Geopetals measured in the coral rudstone in the east section south of the mine opening, show that the measured dip represents the original synsedimentary slope. Carbonate deposition occurred intermittently during periods of volcanic quiescence between episodes of volcaniclastic deposition. There is a clear fining-westward pattern in grain size between the two measured sections in all facies (Fig. 4), confirming a more proximal marine setting for the east section.

6.1 Interpretation of Facies I

This facies represents the incipient development of a carbonate ramp banked against the flank of a volcano. Because the dip is 9° SSW and the two sections are 65 m apart lying on strike, the absolute difference in depth between the east and the west sections was close to 10 m. Both macrofossils and thin section analysis indicate open marine conditions. Pectinids and the abundant rhodolith debris suggest transportation from an offshore source, as typical of Pliocene carbonates in the Gulf of California (Eros *et al*., 2006).

The foraminifers are all benthic and indicate a relatively shallow depth, as does the unusually poor *Bichordites*/*Dactyloidites* ichno-assemblage emplaced towards the top of Facies I on the west side. Microfacies analysis demonstrates a high proportion of micrite in both sections and this suggests that the layer was deposited below normal wave base. Many bioclastic grains have micritized rims and envelopes indicating a long residence time under stable conditions. The *Bichordites*/*Dactyloidites* ichno-assemblage is commonly related to a soft substrate in high-energy environments (Pickerill *et al*., 1993; Gibert and Goldring, 2008). Thus, this facies most likely was deposited above storm wave-base, but below normal wave-base in an environment occasionally disturbed by storms.

6.2 Interpretation of Facies II

The basal layer above Facies I is a typical example of a surtseyan deposit (e.g. it originated from a coeval volcanic eruption and settled out of the watercolumn, hence a tuff showing no erosive base). Imbrication of clasts in the slightly coarser, but still thinly bedded tuffites immediately above, together with erosive bases also in the conglomeratic tuffite, indicate transport. These represent good examples of subaquous density flows as defined by Mulder and Alexander (2001). The flows correspond to debris flows and hyperconcentrated density flows, including grainflows. The presence of trace fossils below and above shows that all the flows occurred in a marine setting and the transition from debris flows through hyperconcentrated flow into grainflows signifies an increasing ingress of water and marine sediments into the flows. These flows originated by

reworking of volcaniclastic flows and surtseyan deposits in a lava apron and may have been created by collapse of the coastal margin, a submarine volcanic cone, or the submarine parts of a lava delta. Oyster-encrusted boulders are typical of Recent and ancient beaches (Hayes *et al*., 1993; Johnson and Baarli, 2012). Most likely, these Miocene boulders were picked up and swept into a flow originating close to or over-running the shore.

6.3. Interpretation of Facies III

Facies III represents a period of renewed carbonate production and quiescence expressed by the lower carbonate bed, interrupted by two episodes of density flows originating from shallower positions. The large bioeroded block found on the east side in the lower carbonate bed preserves *Gastrochaenolites torpedo* and *G. lapidicus* bioerosion, indicating it came from a site with a low to zero sedimentation rate in a shallow setting (Bromley and Aasgard, 1993). The shear size of the block may indicate collapse of a shallow, nearby, underwater cliff, sea stack, or channel wall into the site of deposition below.

Like the conglomeratic tuffite debris flow below, belonging to Facies II, the coral rudstone also is interpreted as a debris flow. In contrast to the conglomeratic tuffites originating to the NNE, these coral cobbles are clearly transported from the ENE and the bed has a strongly erosive base. This flow also appears to have cannibalized parts of the first debris flow and incorporated basalt cobbles from it.

6.4. Interpretations of Facies IV

This facies consists of unsorted coarse volcaniclastic sand with a high carbonate content that reflects a lack of winnowing by waves or currents and the strong influence both from volcaniclastic sources on land and adjacent production of marine carbonates. The most common fossil group is echinoids and their associated traces, *Bichordites* isp. These, together with the bivalve *Pinna* sp., indicate a soft substrate.

Immediately overlying is a 7-m-thick basalt flow showing that the absolute depth for both sections was at least 7 m. Because the 20^{o} dip is close to the original slope of the synsedimentary sea bottom, there was more than a 20 m difference in depositional depth between the east and west sides of the island. Thus, the section on the west side may have been deposited at comparable depths or slightly deeper than Facies I. However, the amount of basalt sand is vastly higher than in Facies I, so it was probably in a more proximal position relative to the shore.

7. DISCUSSION

7.1. Discussion of Facies I

Rhodolith grains are dominant among the bioclastic grains from Facies I. A few whole rhodoliths are present, but rare. The flank of a volcano and the steep and unstable front of an active lava delta would not be favourable for an organism that requires occasional rotation like rhodoliths. Indeed, looking at the modern occurrences of living rhodoliths at

Porto Santo, we find they live on the relatively level bottom of the bay and not along the steep shoreface. Near-shore fossil rhodoliths mainly are transported onshore, as found at Ilhéu de Cima (Johnson *et al.*, 2011), although they may also occur in limited numbers in depressions on narrow shelves (Santos *et al*., 2012c). Open marine platforms occasionally swept by storms are among the most commonly interpreted settings for rhodoliths (Martin *et al*., 1993). Therefore, a major influx of rhodolith material from offshore banks is most likely.

The study site is situated on the south side of Ilhéu de Baixo and is further sheltered by the main island of Porto Santo, an island that was considerable larger when it was formed during Miocene time (Schmidt and Schmincke, 2002). The micritized rims and envelopes on bioclastic grains indicate generally stable conditions. Also, the presence of trace fossils in the upper parts of the bed shows they represent primary deposits. This distal part of the volcanic flank, therefore, must have experienced longer periods of volcanic quiescence.

The *Bichordites*/*Dactyloidites* ichno-assemblage present at the top of Facies I is commonly connected to high-energy environments, specifically storm facies (Johnson *et al.,* 2012). It most likely records the very occasional storm or hurricane that typically approached from the SSE (Johnson *et al.,* 2011). The same authors argued that hurricanes probably were more frequent during Miocene time on Porto Santo, although only seldom experienced in the region during Recent times (Vaquero *et al.,* 2008). Thus, this facies was deposited in a calm environment only very occasionally disturbed by storms.

The foraminifer species *Amphistegina lessonii* d'Orbigny was reported from Ilhéu de Baixo by Silva (1959). This is a species that requires high light and moderate energy conditions. It has an optimum depth range between 5 and 30 m (Hallock and Glenn, 1986). This evidence supports that the mined layer was originally deposited below normal wave-base at moderate depths, but above storm-wave-base.

This facies includes 16 to 17 % basalt grains, showing there was a steady influx of volcaniclastic material that might have contributed to the soft substrate. Many carbonate-producing organisms have difficulties tolerating a high influx of insoluble clasts. Mobile animals, i.e. those with a morphology adapted to an unstable substrate with low-light levels, and self-cleaning organisms are best adapted for such a setting (Wilson and Lokier, 2002). The above-mentioned authors found that echinoderms, worms, large benthic foraminifers, some corals, large molluscs, and coralline algae were frequently found in areas with high volcaniclastic input. This assemblage is closely comparable to the organisms present in Facies I.

7.2. Discussion of Facies II

All flows discussed are gravity driven and both surtseyan tuffs and the density flows are typical of the distal parts of lava deltas in pre-emergent and emergent volcanic settings (Watton *et al.,* 2013). Coarse-grained density flows in Facies II are predominant on the east side, while the finer flows mainly occur at the west side. This signifies settling of flows and increasing incorporation of water and marine sediments into the flows with increased distance from the source and distance downslope. The density flows may

originate at the water's edge due to synsedimentary wave-induced reworking in the shore zone, or as described by Schneider *et al.* (2004) from the Mio-Pliocene of Gran Canaria, as reworking of volcanic-debris avalanches that entered the sea. They may also result from secondary reworking and slumps during delta-front collapse (Watton *et al*., 2013). Because many of the flows in Facies II (Fig. 3C, left of arrow a) terminate closer to the source, surtseyan deposits interspersed with undisturbed carbonate beds are most common distally. In this case, the section is terminated by a 7-m-thick lava flow indicating that the site probably was at the transition between a prodelta and the distal delta front.

7.3. Discussion of Facies III

The fact that few corals appear in an upside-down position probably reflects a limited amount of turbulence within the flow. This debris flow arrived with coral heads from another direction than those in Facies II. It terminates towards the northwest and the cross-section indicates a transport direction from the northeast. This suggests that a reef was building out in that direction and the coral rudstone density bed signifies partial reef collapse and slope failure with final deposition in a fore-reef environment. Some corals are able to tolerate a nearly continuous influx of volcaniclastic influx (Wilson and Lokier, 2002; Lokier *et al.,* 2009) but major reef development may have required a longer period without major volcaniclastic influx and stable slopes between lava deltas. The reef, itself, supported a rich fauna both in terms of corals and bioeroders.

Chaetetids are often associated with cryptic environments such as submarine caves within reefs or dimly lighted fore-reefs (Reitner and Engeser, 1987). These sponges commonly occur in the coral rudstone. However, chaetetids also are found encrusting the large basalt boulder (Fig. 8D) that was eroded from the volcanic debris flow below. Thus, it is difficult to know if the sponges inhabited the reef or came from another environment upslope, farther to the north.

7.4.Discussion of Facies IV

Census counts show that the coral patches in Facies IV are very strongly bioeroded, while encrusting bivalves show little bioerosion. This may mean that the corals were transported into this environment and later became encrusted by the bivalves *in situ*. The facies appears to represent a quiet-water environment probably protected by a newly developed reef towards the east where the corals originated. The fauna is mixed, but many elements represent near-shore organisms that cement themselves to a hard substrate. The over-steepening of the bottom of this bed was due to the progradation of a lava delta consequential to the buildup of volcaniclastic density flows down the slope as they gradually increased the steepness of the island's flank. Thus, this facies developed in a more proximal position to the shore than Facies I.

7.5. Preservation of a carbonate ramp in a delta-front setting

Carbonates from volcaniclastic environments are well described by Wilson and Lokier (2002) from Neogene deposits of Indonesia. However, their study looks at lava delta-front patch reefs and compared them to carbonate platforms with terrigenous influx. The present Ilhéu de Baixo study deals with an incipient carbonate ramp formed at a relatively high angle at the foot of a delta front punctuated by volcaniclastic density flows and terminated by a lava flow. Where patch reefs have sufficient time to develop, they can be predicted to stand as positive features deflecting volcaniclastic density flows that divert around them. It is likely a ramp is more apt to be buried. Also, where flows are frequent enough, the carbonates may be incorporated into flows with little trace of the original bed or a chance to development into a ramp.

Only the basal carbonate bed and the topmost carbonate rich-layer in Facies IV include trace fossils preserved near the top. The tuffitic hyper-concentrated density flows occurring in the middle of the sections contain considerable amounts of carbonate sediment and must have eroded deeply into the carbonate beds below. The maker of the trace fossils, *Bichordites* isp., burrows to a depth of 15 cm below the seafloor (Bromley and Asgaard, 1975). *Dactyloidites* isp. is made by a worm-like animal, and burrows very superficially just below the sediment surface (Gibert *et al.,* 1975). Any trace of such organisms that lived in the surface layers would likely be removed by a passing density flow at the same time as shells and other organic debris were incorporated. Basaltic flows often "bake" and recrystallize the topmost layer of a limestone destroying primary structures, although the effect is limited to the contact zone. This is in contrast to surtseyan deposits that may promote the preservation of carbonates. If thick enough, surtseyan deposits should protect carbonate beds from erosion by subsequent density

flows. Thus, explosive eruptions have the general potential to help preserve distal carbonate deposits (Fig. 9).

8. CONCLUSIONS

Porto Santo in the Madeira Archipelago is an oceanic island that retains an array of carbonate beds intercalated between basalt flows and/or volcaniclastic sediments indicating a fascinating diversity of dynamic environments. A satellite islet to Porto Santo, Ilhéu de Baixo, adds to this diversity. Six core findings underscore the results of this study in the context of active volcanism and slope failure on the flank of a Middle Miocene oceanic island.

1. The investigated sections consist of carbonate beds incorporated within the apron of an active volcano on an oceanic island. The carbonates were deposited during periods of relative volcanic quiescence, but punctuated by influx of volcaniclastic materials, either as primary surtseyan deposits or as subaqueous density flows reworked from surtseyan deposits and volcaniclastic flows.
2. Initially, an incipient carbonate ramp was emplaced on the prodelta to distal delta front under the influence of open-marine conditions. This interval of carbonate sediments was deposited below normal-wave base, but above storm-wave base. From an ecological perspective, bioclasts in this facies are dominated by crushed bits of rhodoliths (coralline red algae), which account for 13% of the whole or 51% of all identifiable bioclasts. The rhodolith material was most likely transported shoreward

from an offshore bank. Other bioclasts feature contributions from bivalves, gastropods, corals, echinoderms, bryozoans, and foraminifers. In addition, trace fossils created by echinoderm and worm-like organisms are present, reflecting on organisms tolerant of a steady influx of volcaniclastic material.

3. Progradation of the lava delta front mainly represented by piles of hyaloclastites deposited as density flows contributed to local steepening of the sea floor and the introduction of large bioeroded and encrusted carbonate blocks from a nearshore collapse.
4. Presence of a parent reef is indicated by a coral rudstone density flow generated by the collapse of an upslope structure. This density flow originated from the east, while the delta front advanced from a NNE direction.
5. Ending the sequence, carbonate-rich volcaniclastic sand accumulated in a quiet fore-reef environment sufficiently stable to support burrowing by echinoderms. The deposit also includes coral colonies transported downslope and encrusted after transport by *in situ* bivalves. The entire section is terminated by a 7-m-thick flow of pillow lava that indicates the minimum water depth for the preceding deposit.

This study shows how carbonate beds embanked on the margins of active volcanic islands are subject to different outcomes. Carbonates are at strong risk of being reworked and incorporated into density flows of various kinds, to the extent that any trace of their former development as distinct bed forms is erased. Alternatively, surtseyan deposits and less erosive lava flows may help to preserve carbonate beds that accumulated during intervals of relative volcanic quiescence.

ACKNOWLEDGEMENTS

During fieldwork in June 2009, Johnson was supported by a travel grant from the Class of 1945 Faculty World Fellowship from Williams College. Santos received financial support from the Spanish Ministry of Science and Technology (Juan de la Cierva subprogram, Ref: JCI-2008-2431) and the Junta de Andalucía (Spanish government) to the Research Group RNM316 (Tectonics and Palaeontology). During fieldwork in June 2010, all participants received support from grant CGL2010-15372-BTE from the Spanish Ministry of Science and Innovation to project leader Eduardo Mayoral (University of Huelva). The Portuguese Navy provided transportation to and from Ilhéu de Baixo during all visits to this and others islets. We are grateful to Michael Blandy for insight on the Blandy Brothers mine and its history. Finally, the manuscript was much improved by helpful reviews and detailed comments by Davide Bassi, Ricardo Ramalho, and the journal's Editor-in-Chief, Ian Somerville.

REFERENCES

Ávila, S.P., Madeira, P., Zazo, C., Kroh, A., Kirby, M., Silva, C.M., Cachão, M., Frias Martins, A.M. 2009. Palaeoecology of the Pleistocene (MIS 5.5) outcrops of Santa Maria Island (Azores) in a complex oceanic tectonic setting. *Palaeogeography, Palaeoclimatology, Palaeoecology* **274**, 18-31.

Best, M.W., Boekschoten, G.J. 1982. On the coral fauna in the Miocene reef at Baixo, Porto Santo (Eastern Atlantic). *Netherlands Journal of Zoology* **32**, 412-418.

Boekschoten, G.J., Best, M.W. 1981. *Pocillopora* in the Miocene reef at Baixo, Porto Santo (Eastern Atlantic). *Proceedings Koninklijke Nederlandse Adademie van Wetenschappen, Series B* **84**, 13-20.

Bromley, R.G., Asgaard, U. 1975. Sediment structures produced by a spatangoid echinoid: a problem of preservation. *Bulletin geological Society Denmark* **24**, 261-281.

Bromley, R.G., Aasgard, U. 1993. Two bioerosion ichnofacies produced by early and late burial associated with sea-level change. *Geologische Rundschau* **82**, 276-280.

Cachão, M., Rodrigues, D., Silva, C.M. da, Mata J. 1998. Biostratigrafia (Nanofósseis calcários) e interpretação paleoambiental do Neogénico de Porto Santo (Madeira), Dados preliminares. *Comunicações do Instituto Geológico e Mineiro* **84**, A185-A188.

Chevalier, J.P. 1972. Les Scléractiniaries du Miocéne de Porto Santo (archipel de Madeira). *Annales de Paléontologie des Invertébrés* **58**, 141-160.

Darwin, C. 1839. Journal and Remarks, 1832-1836. In: FitzRoy, R. (Ed.), *Narrative of the Surveying Voyages of His Majesty's Ships Adventure and Beagle Between the Years 1826 and 1836,* Volume 3, Henry Colburn, London, 615 p.

Darwin, C. 1844. *Geological Observations on the Volcanic Islands Visited During the Voyage of the H.M.S. Beagle*. Smith, Elder & Co., London, 175 p.

Eros, J.M., Johnson, M.E., Backus, D.H. 2006. Rocky shores and development of the Pliocene-Pleistocene Arroyo Blanco Basin on Isla Carmen in the Gulf of California, Mexico. *Canadian Journal of Earth Sciences* **43**, 1149-1164.

Ferreira, M.P. 1996. *Carta Geolólogica de Portugal, Folha da Ilha de Porto Santo.* Ministério da Economia, Instituto Geológico e Mineiro, Portugal, Escala 1:25,000.

Gibert, J.M. de, Martinell, J., Doménech, R. 1995. The rosetted feeding trace fossil *Dactyloidites ottoi* (Geinitz) from the Miocene of Catalonia. *Geobios* **28**, 769-776.

Gibert, J. M. de, Goldring, R. 2008. Spatangoid-produced ichnofabrics (Bateig Limestone, Miocene, Spain) and the preservation of spatangoid trace fossils. *Palaeogeography, Palaeoclimatology, Palaeoecology* **270**, 299-310.

Hallock, P., Glen, E.C. 1986. Larger foraminifera: A tool for paleoenvironmental analysis of Cenozoic carbonate depositional facies. *Palaios* **1**, 55-64.

Hayes, M.L., Johnson, M.E., Fox, W.T. 1993. Rocky-shore biotic associations and their fossilization potential: Isla Requeson (Baja California Sur, Mexico). *Journal of Coastal Research* **9**, 944-957.

Johnson, M.E., Baarli, B.G. 2012. Development of intertidal biotas through Phanerozoic time, pp. 63-128. In: *Earth and Life: Global Biodiversity, Extinction Intervals and Biogeographic Perturbations Through Time.* Talent, J.A. (ed), Springer Science and Media, Dordrecht, 63-128.

Johnson, M.E., Silva, C.M. da, Santos, A., Baarli, B.G., Cachão, M., Mayoral, E.J., Rebelo, A.C., Ledesma-Vázquez, J. 2011. Rhodolith transport and immobilization on a volcanically active rocky shore: Middle Miocene at Cabeço das Laranjas on

Ilhéu de Cima (Madeira Archipelago, Portugal). *Palaeogeography, Palaeoclimatology, Palaeoecology* **300**, 113-127.

Johnson, M.E., Baarli, B.G., Cachão, M., Silva, C.M. da, Ledesma-Vázquez, J., Mayoral, E.J., Ramalho, R.S., Santos, A. 2012. Rhodoliths, uniformitarianism, and Darwin: Pleistocene and Recent carbonate deposits in the Cape Verde and Canary archipelagos. *Palaeogeography, Palaeoclimatology, Palaeoecology* **329-330**, 83-100.

Lokier, S.W., Wilson, M.E.J., Burton, L.M. 2009. Marine biota response to clastic sediment influx: a quantitative approach: *Palaeogeography, Palaeoclimatology, Palaeoecology* **281**, 25–42.

Martin, M.M., Braga, J.C., Konishi, K., Pigram, C.J. 1993. A model for the development of rhodoliths on platforms influenced by storms: Middle Miocene carbonates of the Marion Plateau (Northeastern Australia). In: *Proceedings Ocean Drilling Program* McKenzie, J.A., Davies, P.J., Palmer-Julson, A. (eds.), **133**, 455-465.

Meco, J., Scaillet, S., Guillou, H., Lomoschitz, A., Carlos Carracedo, J., Ballester, J., Betancort, J. F., Cilleros, A. 2007. Evidence for long-term uplift on the Canary Islands from emergent Mio-Pliocene littoral deposits: *Global and Planetary Change* **57**, 222-234.

Mitchell-Thomé, R.C. 1974. The sedimentary rocks of Macaronesia. *Geologische Rundschau* **63**, 1179-1216.

Mulder, T., Alexander, J. 2001. The physical character of subaqueous sedimentary density flows and their deposits. *Sedimentology* **48**, 269-299.

Pickerill, R.K., Donovan, S.K., Dixon, H.L. 1993. The trace fossil *Dactyloidites ottoi* (Geinitz, 1849) from the Neogene August Town Formation of south-central Jamaica. *Journal of Paleontology* **67**, 1070–1074.

Reitner, J., Engeser, T.S. 1987. Skeletal structures and habitats of Recent and fossil *Acanthochaetetes* (subclass Tetractinomorpha, Demospongia, Porifera). *Coral Reef* **6**, 13-18.

Santos, A., Mayoral, E.J., Silva, C.M. da, Cachão, M., Johnson, M.E., Baarli, B.G. 2011. Miocene intertidal zonation on a volcanically active shoreline: Porto Santo in the Madeira Archipelago (Portugal). *Lethaia* **45**, 26-32.

Santos, A., Mayoral, E., Johnson, M.E., Baarli, B.G., Cachão, M., Silva, C.M. da, Ledesma-Vásquez, J. 2012a. Extreme habitat adaptation by boring bivalves on volcanically active paleoshores from North Atlantic Macaronesia. *Facies* **58**, 325-338.

Santos, A., Mayoral, E., Baarli, B.G., Silva, C.M. da, Cachão, M., Johnson, M.E. 2012b. Symbiotic association of a pyrgomatid barnacle and a coral from a volcanic middle Miocene shoreline (Porto Santo, Madeira Archipelago, Portugal). *Palaeontology* **55**, 173-182.

Santos, A.G., Mayoral, E., Johnson, M.E., Baarli, B.G., da Silva, C.M., Cachão, M.D., Ledesma-Vázquez, J. 2012c. Basalt mounds and adjacent depressions attract contrasting biofacies on a volcanically active Middle Miocene shoreline (Porto Santo, Madeira Archipelago, Portugal). *Facies* **58**, 573-585.

Schmidt, R., Schmincke, H.-U. 2002. From seamount to oceanic island, Porto Santo, Central East-Atlantic. *International Journal of Earth Sciences (Geologische Rundschau)* **91**, 594-614.

Schneider, J.-L., Pérez Torrado, F.J., Gimeno Torrentec, D., Wassmerd, P., del Carmen Cabrera Santanab, M., Carracedoe, J. C. 2004. Sedimentary signatures of the entrance of coarse-grained volcaniclastic flows into the sea: the example of the breccia units of the Las Palmas Detritic Formation (Mio-Pliocene, Gran Canaria, Eastern Atlantic, Spain). *Journal of Volcanology and Geothermal Research* **138**, 295-323.

Scholle, R.P., Bebout, D.G., Moore, C.H. (eds.) 1983. *Carbonate Depositional Environments*, Memoir 33. American Association of Petroleum Geologists, Tulsa, Oklahoma, 708 p

Silva, G.H. da 1959. Fósseis do Miocénico marinho da Ilha de Porto-Santo. *Memórias e Notícias, Museu Mineralógico e Geológico da Universidade de Coimbra* **48**, 1-22.

Soja, C.M. 1993. Carbonate platform evolution in a Silurian oceanic island: A case study from Alaska's Alexander Terrane. *Journal of Sedimentary Petrology* **63**, 1078-1088.

Van der Plas, L., Tobi, A.C. 1965. A chart for judging the reliability of point counting results. *American Journal of Science* **263**, 87-90.

Vaquero, J.M., García-Herrera, Wheeler, D., Chenoweth, M., Mock, C.J. 2008. A historical analog of 2005 Hurricane Vince. *Bulletin of the American Meteorological Society* **85**, 191-201.

Watton, T.J., Jerram, D.A., Thordarson, T., Davies, R.J. 2013, Three-dimensional lithofacies variations in hyaloclastite deposits. *Journal of Volcanology and Geothermal Research* ***250***, 19-33.

Wilson, J.L. 1975. *Carbonate Facies in Geologic History.* Springer-Verlag, New York, 471 p.

Wilson, M.E.J., Lokier, S.W. 2002. Siliciclastic and volcaniclastic influences on equatorial carbonates: insights from the Neogene of Indonesia. *Sedimentology* **49**, 583–601.

Zazo, C., Goy, J. L., Dabrio, C. J., Soler, V., Hillaire-Marcel, C., Ghaleb, B., González-Delgado, J. A., Bardají, T., Cabero, A. 2007. Quaternary marine terraces on Sal Island (Cape Verde archipelago): *Quaternary Science Reviews* **26**, 876-893.

Zazo, C., Goy, J. L., Hillaire-Marcel, C., Dabrio, C. J., González-Delgado, J. A., Cabero, A., Bardají, T., Ghaleb, B., Soler, V. 2010. Sea level changes during the last and present interglacials in Sal Island (Cape Verde archipelago). *Global and Planetary Change* **72**, 302-317.

Zazo, C., Goy, J.L., Hillaire-Marcel, C., Gillot, P., Soler, V., González, J.A., Dabrio, C.J., Ghaleb, B. 2002. Raised marine sequences of Lanzarote and Fuerteventura revisited—a reappraisal of relative sea-level changes and vertical movements in the eastern Canary Islands during the Quaternary. *Quaternary Science Reviews* **21**, 2019–2046.

Table 1. Point-count data from mine pillar 1a.

Blandy Brothers 1a	Run 1		Run 2		Run 3		Average
	No.	%	No.	%	No.	%	%
Matrix	164	41	163	39	167	42	41
Void	65	16	90	21	57	14	17
Red algae	57	14	54	13	51	13	13
Bivalves	17	4	12	3	22	6	4
Gastropods	2	0.5	2	0,5	6	2	1
Corals	4	1	10	2	10	3	2
Foraminifers	12	3	8	2	10	3	3
Echinoderms	12	3	9	2	4	1	2
Bryozoans	2	0.5	2	0.5	4	1	1
Undetermined	3	1	3	1	3	1	1
Basalt	64	16	70	17	66	15	16
Total	402	100	423	101	400	101	

Bioclast counts	Run 1		Run 2		Run 3		Average
	No.	%	No.	%	No.	%	%
Red algae	57	52	54	54	51	46	51
Bivalves	17	16	12	12	22	20	16
Gastropods	2	2	2	2	6	5	3
Corals	4	4	10	10	10	9	8
Foraminifers	12	11	8	8	10	9	9
Echinoderms	12	11	9	9	4	4	8
Bryozoans	2	2	2	2	4	4	3
Serpulids	0		0		0		0
Undetermined	3	3	3	3	3	3	3
Total	109	101	100	100	110	100	101

Table 2. Point-count data from mine pillar 1b.

Blandy Brothers 1a	Run 1		Run 2		Run 3		Average
	No.	%	No.	%	No.	%	%
Matrix	193	48	197	48	197	48	48
Void	55	14	61	15	59	14	14
Red algae	41	10	58	14	48	12	12
Bivalves	20	5	21	5	23	6	5.3
Gastropods	1	0.2			2	0.5	0.2
Corals	8	2	5	1.2	8	2	1.7
Foraminifers	5	1.2	4	1	6	1.3	1.2
Echinoderms	6	1.5	7	1.7	6	1.3	1.5
Bryozoans	3	0.7	1	0.2			0.3
Serpulids	1	0.2					0.1
Undetermined	2	0.4	2	0.5			0.9
Basalt	66	16.5	54	13	59	14.5	14.7
Total	401	99.7	410	99.6	408		99.9

Bioclast counts	Run 1		Run 2		Run 3		Average
	No.	%	No.	%	No.	%	%
Red algae	41	49	58	59	48	52	53
Bivalves	20	24	21	21	23	25	23
Gastropods	1	1			2	2	1
Corals	8	10	5	5	8	9	8
Foraminifers	5	6	4	4	6	6	5
Echinoderms	6	7	7	7	6	6	6.7
Bryozoans			1	1			0.3
Serpulids	1	1					0.3
Undetermined	2	2	2	2			0.6
Total	84	100	98	99	93	100	97.9

Table 3. Point-count data from mine pillar 2.

Blandy Brothers 1a	Run 1		Run 2		Run 3		Average
	No.	%	No.	%	No.	%	%
Matrix	229	57	253	62	220	51	57
Void	16	4	20	5	16	4	4
Red algae	68	17	45	11	68	16	15
Bivalves	18	5	24	6	31	7	6
Gastropods	4	1	1	0.2	7	1.5	1
Corals	10	3	7	1.7	21	5	3
Foraminifers	8	2	11	2.7	14	3	2.5
Echinoderms	3	0.6	5	1	8	2	1.2
Bryozoans			6	1.5	14	3	1.5
Serpulids					3	0.6	0.2
Undetermined	2	0.5					0.2
Basalt	41	10	38	9	31	7	8.5
Total	399	100.1	410	100.1	433	100.1	100.1

Bioclast counts	Run 1		Run 2		Run 3		Average
	No.	%	No.	%	No.	%	%
Red algae	68	61	45	45	68	41	49
Bivalves	18	16	24	24	31	19	20
Gastropods	4	4	1	1	7	4	3
Corals	10	9	7	7	21	13	9.5
Foraminifers	8	7	11	11	14	8	8.5
Echinoderms	3	3	5	5	8	5	4
Bryozoans			6	9	14	8	5.5
Serpulids					3	2	0.5
Undetermined							
Total	111	100	99	99	166	100	100

Table 4. Point-count data from mine pillar 3.

Blandy Brothers 1a	Run 1		Run 2		Run 3		Average
	No.	%	No.	%	No.	%	%
Matrix	231	58	207	52	215	53	54
Void	33	8	38	10	40	10	9.3
Red algae	64	16	56	14	49	12	14
Bivalves	23	6	24	6	25	6	6
Gastropods	2	0.5	5	1	5	1	0.8
Corals	7	2	8	2	15	4	2.6
Foraminifers	2	0.5	5	1	6	1	0.8
Echinoderms	3	0.8	1	0.3	13	3	1.4
Bryozoans	1	0.2	6	1.5	2	0.5	0.7
Serpulids			2	0.5	1	0.2	0.2
Undetermined					1	0.2	
Basalt	34	8.5	47	12	37	9	10
Total	400	100.5	399	100.3	409	99.9	99.8

Bioclast counts	Run 1		Run 2		Run 3		Average
	No.	%	No.	%	No.	%	%
Red algae	64	63	56	52	49	39	51
Bivalves	23	23	24	22	25	20	22
Gastropods	2	2	5	5	5	4	3.6
Corals	7	7	8	7	15	12	8.5
Foraminifers	2	2	5	5	6	5	4
Echinoderms	3	3	1	1	13	10	4.5
Bryozoans	1	1	6	6	11	9	5
Serpulids			2	2	1	0.7	1
Undetermined					1	0.7	0.3
Total	102	101	107	100	126	100.4	99.9

FIGURE CAPTIONS

Figure 1. Maps at various scales for the eastern part of the North Atlantic Ocean, the Madeira Archipelago, Porto Santo with its satellite islets, and Ilhéu de Baixo showing the location of the limestone mine in the study area.

Figure 2. Maps at different scales for Ilhéu de Baixo and the south end of the island, showing the layout of the Blandy Brothers limestone mine as series of connected underground galleries. The limestone seam continues to the north and south, but the surface on the island above the mine is basalt.

Figure 3. Views of Ilhéu de Baixo and details of the Blandy Brothers limestone mine: A) View of the island's entire east coast from a distance of about 4 km (north-south island length is 2.75 km and elevation at the north end is 178 m above sea level) with box showing area of enlargement in the next photo, B) Near view of the island's south end from a distance of about 2 km (white arrows related to black arrow 1 point to mine portals in the cliff face; black arrow 2 marks a dark-coloured volcaniclastic wedge), C) South end of Ilhéu de Baixo viewed from the west (white arrows "a" and "b" mark the *c.* 8 m stratigraphic interval shown in Fig. 5A starting with the mined calcarenite; dark openings to the left of "a" are mine portals) , D) Outer mine pillar on the east side of the mine is 2.2 m high, E) Interior view of galleries and support pillars (person for scale).

Figure 4. Stratigraphic sections from opposite sides of the Blandy Brothers mine: West side (A) and East side (B).

Figure 5. Thin-section photographs showing a typical assortment of bioclasts and other features: A) Well-rounded rhodolith fragments (rf), basalt fragments (b) and bivalve fragments (bf) are floating in a sparry micritic matrix among voids (v), B) Coralline red algal fragments (notice the micritic envelope, black arrow), C) Longitudinal section of *Textularia* sp., D) Oblique section of *Amphistegina* sp. (f), E) Unidentified rotaliid foraminifer (f).

Figure 6. Volcaniclastic and carbonate facies: A) Surtseyan deposits (1) conformable above the calcarenites of Facies I, and cut by a hyper-concentrated density flow (2); black arrow demarcates the boundary, B) Facies I (light coloured) overlain by Facies II, showing a bedded hyperconcentrated density flow with dish structures at the base (arrow 1) followed by a graded hyperconcentrated flow with encrusted basalt boulders at the top, C) Detail of basalt boulders with encrusting oysters, D) Facies III showing underlying laminated limestone with a large exotic block on the east side (notice the bioerosion, black arrow); a mix of coral-head boulders and basalt boulders are seen in the overlying rudstone, E) Details from Figure D showing the borings *Gastrochaenolites torpedo* (Gt) and G. *lapidicus* (Gl), F) View northwards on west side showing limits of the coral rudstone marked by dashed line (notice the termination towards the north, white arrow; wedge-shaped beds of volcaniclastic density flows occur below the arrow).

Figure 7. Rose diagrams showing orientations of large coral fronds (*Pocillopora madreporacea*) in Facies III: A) West side, B) East side.

Figure 8. Sedimentological details from Facies III and IV: A, bioeroded coral heads from Facies III (arrows [1] show two cross-sections of the bivalve *Jouannetia* sp., the producer of *Gastrochaenolites orbicularis,* [2] points to the ichnofossil *Gastrochaenolites hospitium* infilled with a fossil of its producer *Lithophaga (Leiosolenus)* sp., [3] points to two fragments of chaetetid sponges (notice many basalt clasts show an envelope of coralline calcareous algae), B) The ichnofossil *G. hospitium* with its producer *Lithophaga (Leiosolenus)* sp. in the coral *Cyphastrea* sp., C) The ichnofossil *Gastrochaenolites orbicularis* in *Pocillopora madreporacea*, D) Chaetetid sponge (marked by dashed lines) encrusting on a basalt boulder, E) Facies IV seen from the west side, F) Patch of worn corals encrusted by *Spondylus* sp. (see arrows), G) Overview photo of the study site looking north; the large bedding plane of Facies IV is marked by an arrow.

Figure 9. Diagrammatic sketch to summarize the placement of carbonate facies on the flanks of an active volcano on Ilhéu de Baixo (adapted from Schmidt and Schmincke, 2002, their figs. 13 G and H).

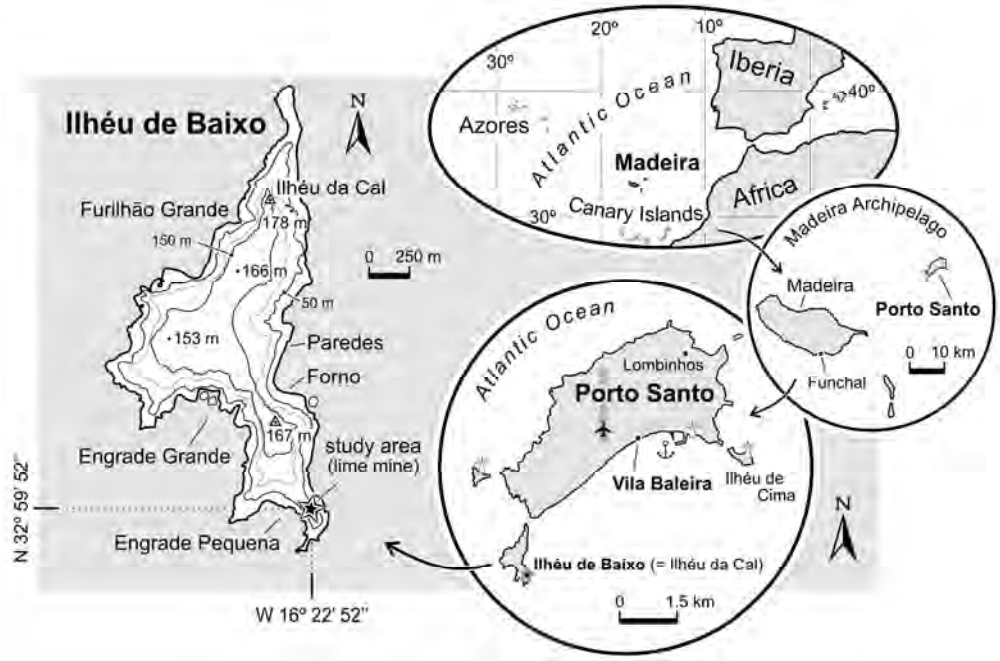

Figure 1. Maps at various scales for the eastern part of the North Atlantic Ocean, the Madeira Archipelago, Porto Santo with its satellite islets, and Ilhéu de Baixo showing the location of the limestone mine in the study area.
171x113mm (300 x 300 DPI)

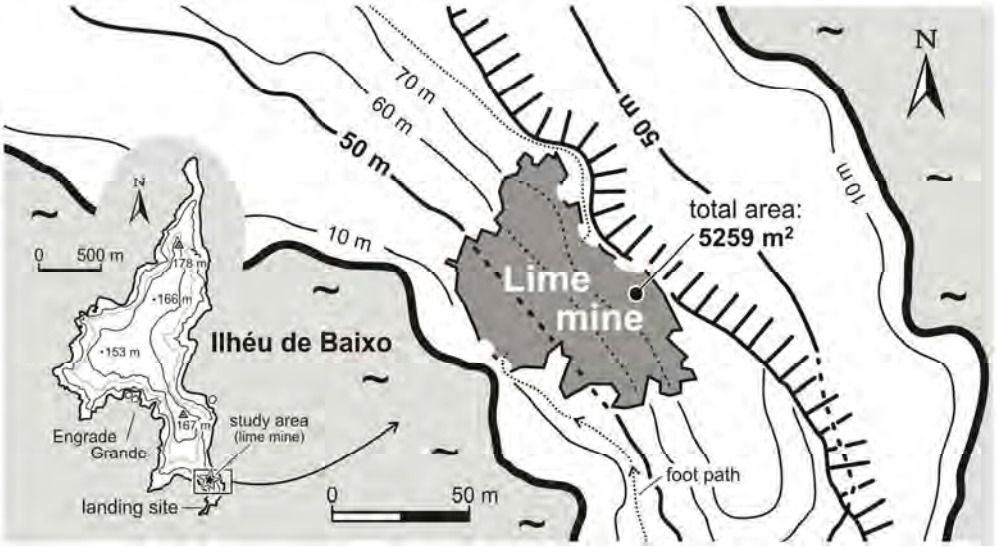

Figure 2. Maps at different scales for Ilhéu de Baixo and the south end of the island, showing the layout of the Blandy Brothers limestone mine as series of connected underground galleries. The limestone seam continues to the north and south, but the surface on the island above the mine is basalt.
166x91mm (300 x 300 DPI)

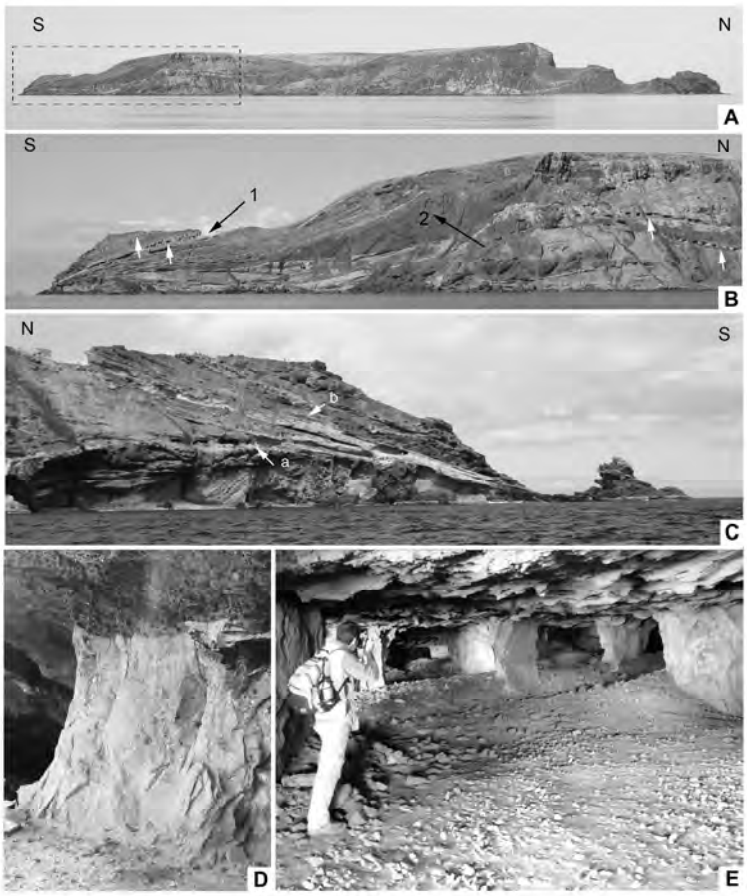

Figure 3. Views of Ilhéu de Baixo and details of the Blandy Brothers limestone mine: A) View of the island's entire east coast from a distance of about 4 km (north-south island length is 2.75 km and elevation at the north end is 178 m above sea level) with box showing area of enlargement in the next photo, B) Near view of the island's south end from a distance of about 2 km (white arrows related to black arrow 1 point to mine portals in the cliff face; black arrow 2 marks a dark-coloured volcaniclastic wedge), C) South end of Ilhéu de Baixo viewed from the west (white arrows "a" and "b" mark the c. 8 m stratigraphic interval shown in Fig. 5A starting with the mined calcarenite; dark openings to the left of "a" are mine portals) , D) Outer mine pillar on the east side of the mine is 2.2 m high, E) Interior view of galleries and support pillars (person for scale).
279x361mm (300 x 300 DPI)

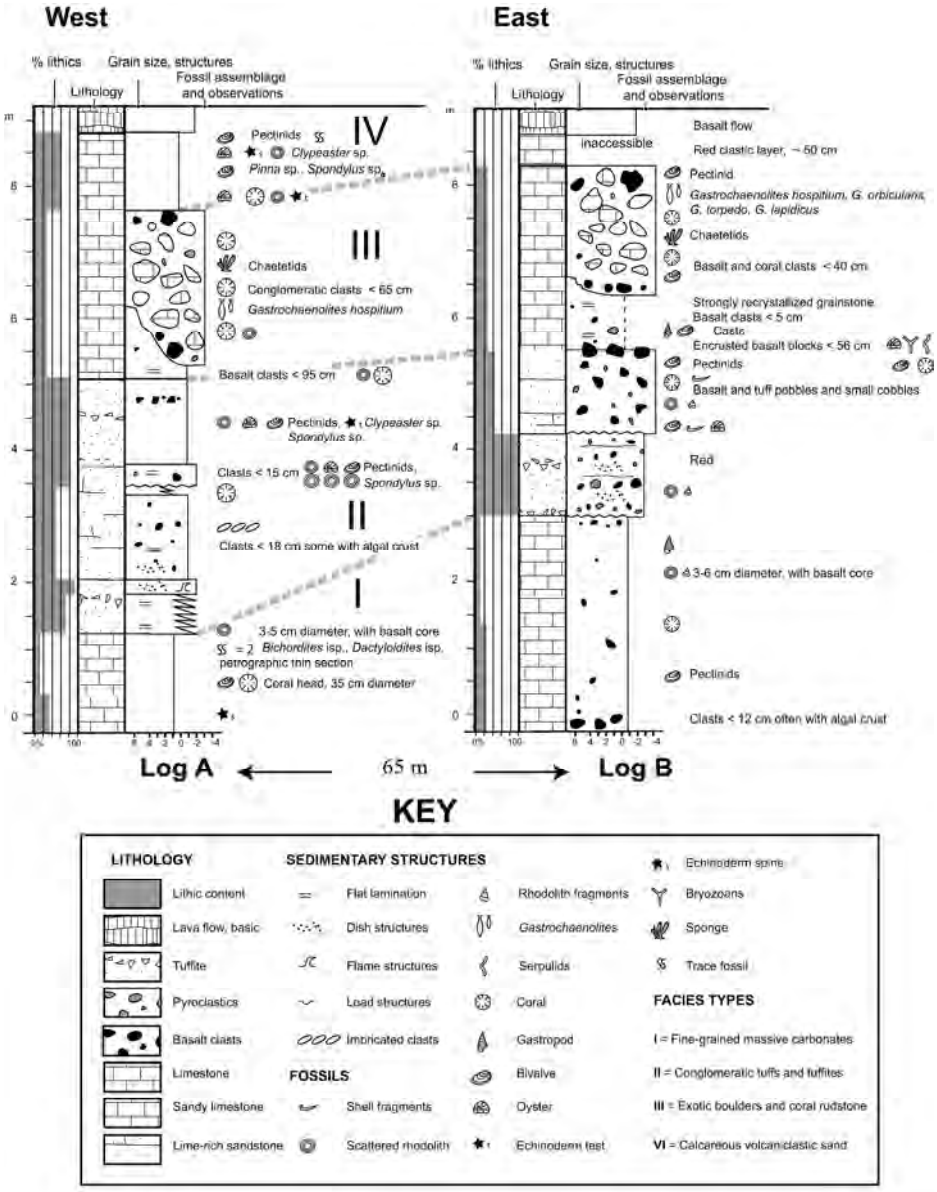

Figure 4. Stratigraphic sections from opposite sides of the Blandy Brothers mine: West side (A) and East side (B).
223x288mm (300 x 300 DPI)

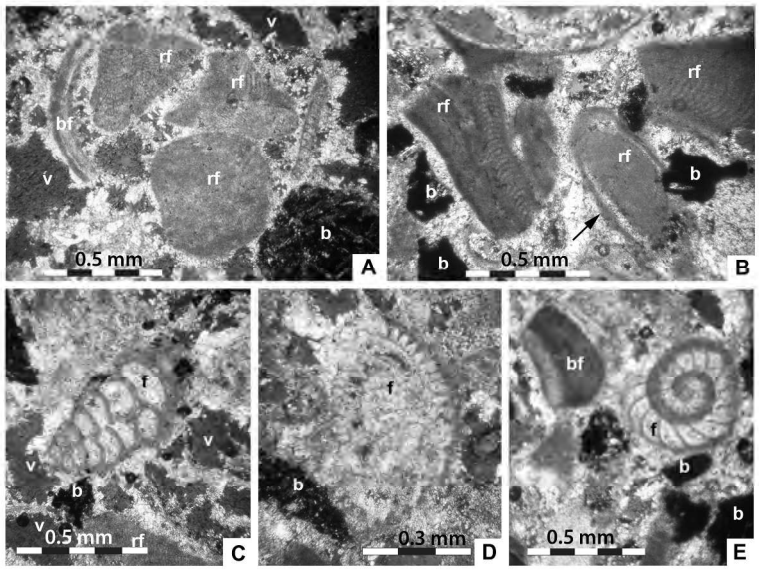

Figure 5. Thin-section photographs showing a typical assortment of bioclasts and other features: A) Well-rounded rhodolith fragments (rf), basalt fragments (b) and bivalve fragments (bf) are floating in a sparry micritic matrix among voids (v), B) Coralline red algal fragments (notice the micritic envelope, black arrow), C) Longitudinal section of Textularia sp., D) Oblique section of Amphistegina sp. (f), E) Unidentified rotaliid foraminifer (f).
279x361mm (300 x 300 DPI)

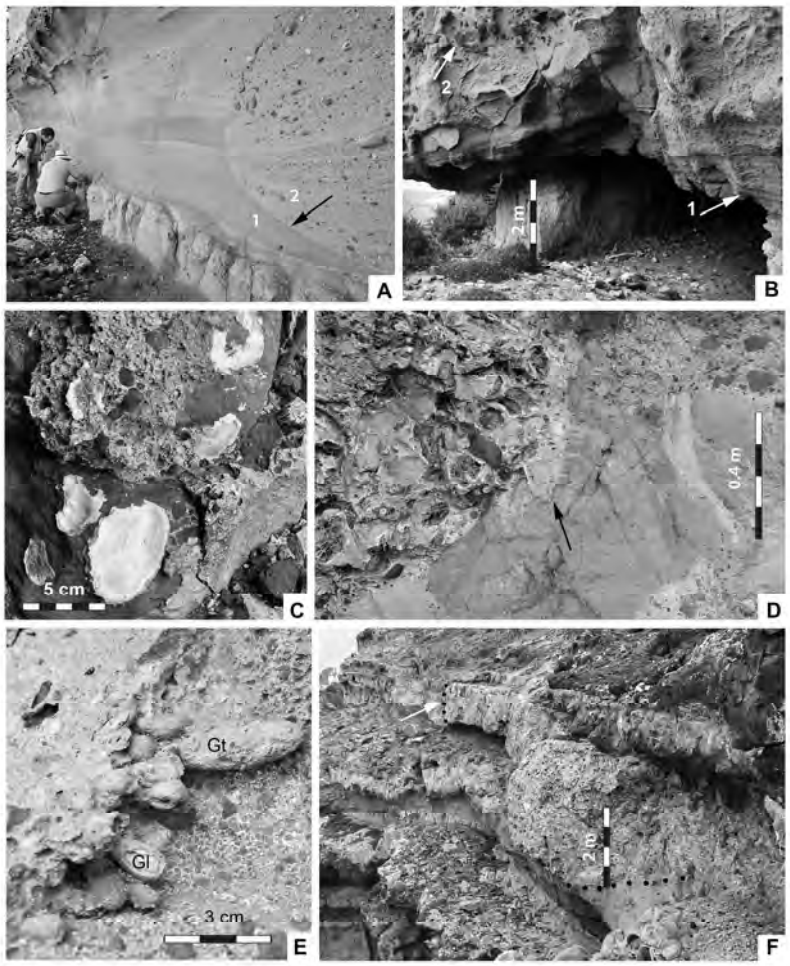

Figure 6. Volcaniclastic and carbonate facies: A) Surtseyan deposits (1) conformable above the calcarenites of Facies I, and cut by a hyper-concentrated density flow (2); black arrow demarcates the boundary, B) Facies I (light coloured) overlain by Facies II, showing a bedded hyperconcentrated density flow with dish structures at the base (arrow 1) followed by a graded hyperconcentrated flow with encrusted basalt boulders at the top, C) Detail of basalt boulders with encrusting oysters, D) Facies III showing underlying laminated limestone with a large exotic block on the east side (notice the bioerosion, black arrow); a mix of coral-head boulders and basalt boulders are seen in the overlying rudstone, E) Details from Figure D showing the borings Gastrochaenolites torpedo (Gt) and G. lapidicus (Gl), F) View northwards on west side showing limits of the coral rudstone marked by dashed line (notice the termination towards the north, white arrow; wedge-shaped beds of volcaniclastic density flows occur below the arrow).
279x361mm (300 x 300 DPI)

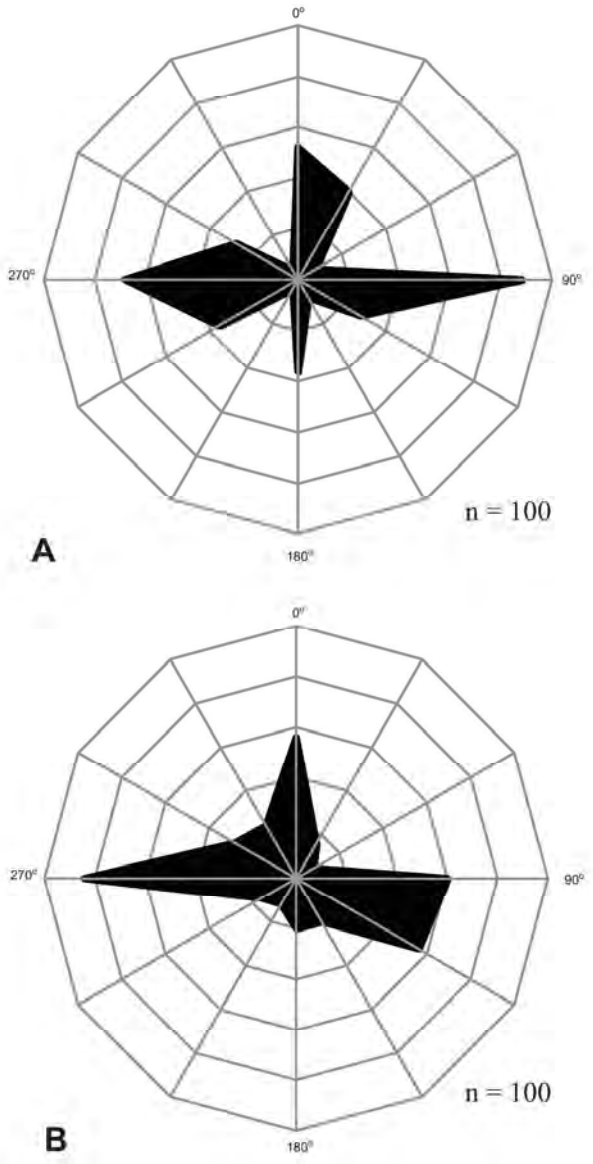

Figure 7. Rose diagrams showing orientations of large coral fronds (Pocillopora madreporacea) in Facies III: A) West side, B) East side.
179x269mm (300 x 300 DPI)

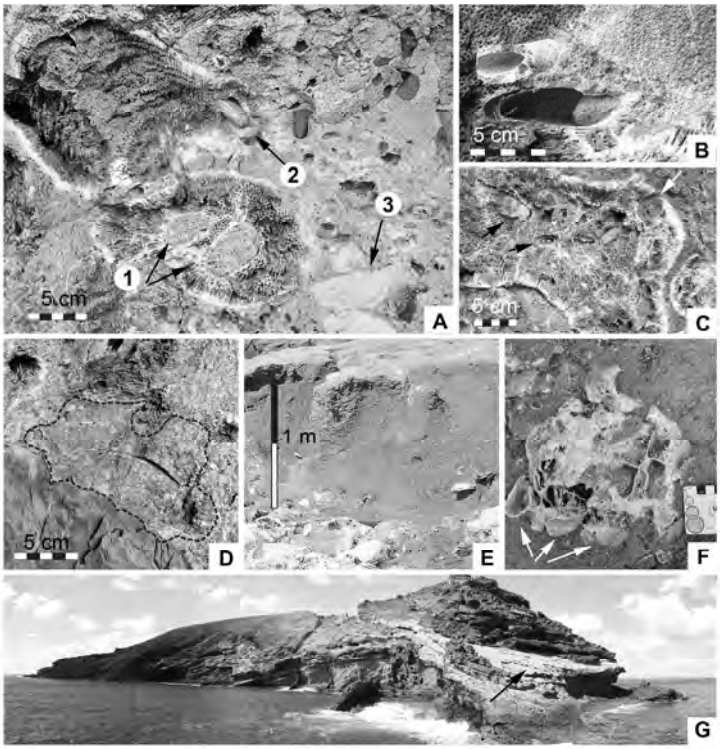

Figure 8. Sedimentological details from Facies III and IV: A, bioeroded coral heads from Facies III (arrows [1] show two cross-sections of the bivalve Jouannetia sp., the producer of Gastrochaenolites orbicularis, [2] points to the ichnofossil Gastrochaenolites hospitium infilled with a fossil of its producer Lithophaga (Leiosolenus) sp., [3] points to two fragments of chaetetid sponges (notice many basalt clasts show an envelope of coralline calcareous algae), B) The ichnofossil G. hospitium with its producer Lithophaga (Leiosolenus) sp. in the coral Cyphastrea sp., C) The ichnofossil Gastrochaenolites orbicularis in Pocillopora madreporacea, D) Chaetetid sponge (marked by dashed lines) encrusting on a basalt boulder, E) Facies IV seen from the west side, F) Patch of worn corals encrusted by Spondylus sp. (see arrows), G) Overview photo of the study site looking north; the large bedding plane of Facies IV is marked by an arrow.
279x361mm (300 x 300 DPI)

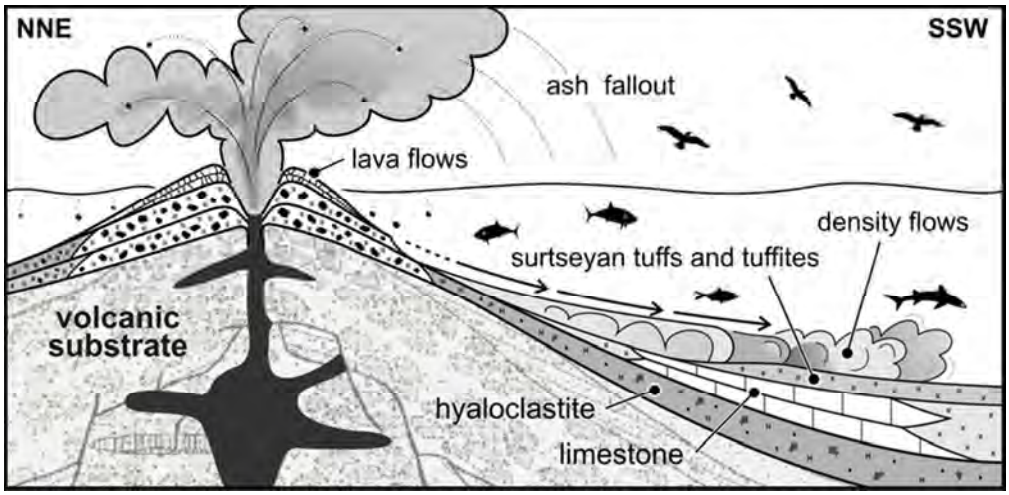

Figure 9. Diagrammatic sketch to summarize the placement of carbonate facies on the flanks of an active volcano on Ilhéu de Baixo (adapted from Schmidt and Schmincke, 2002, their figs. 13 G and H).
64x31mm (300 x 300 DPI)